19th Brazilian Congress of Thermal Sciences and Engineering
November 6th–10th, 2022, Bento Gonçalves - RS - Brazil

ENC-2022-0078
EXPERIMENTAL STUDY ON CONVECTIVE MASS TRANSFER OF HYDROGEN DURING ELECTROLYSIS

Jeferson Diehl de Oliveira
Clauber André Ferasso
Luciane Calabria
Cesar Pandolfi
FSG-University Center, Center of Innovation and Technology, Department of Mechanical Engineering, Os Dezoito do Forte, 2366, Caxias do Sul 95020-472, RS, Brazil
jeferson.oliveira@fsg.edu.br
clauber.ferasso@fsg.edu.br
luciane.calabria@fsg.edu.br
cesar.pandolfi@fsg.edu.br
jacqueline Biancon Copetti
UNISINOS–University of Vale do Rio dos Sinos, Mechanical Engineering Graduate Program, LETEF, Laboratory of Thermal and Fluid Dynamic Studies, Unisinos Avenue, 950, São Leopoldo 93022-750, RS, Brazil
jcopetti@unisinos.br

Elaine Maria Cardoso
UNESP—São Paulo State University, Post-Graduation Program in Mechanical Engineering, Av. Brasil, 56, 15385-000 Ilha Solteira, SP, Brazil
elaine.cardoso@unesp.br

Lirio Schaeffer
UFRGS—Federal University of Rio Grande do Sul, Post-Graduation Program in Mining, Materials, And Metallurgical Engineering, PPG3M, Mechanical Transformation Laboratory LdTM, 91501-970, Porto Alegre, RS, Brazil
schaefer@ufrgs.br

Abstract. *This investigation is devoted to analyzing hydrodynamic behavior and mass transfer performance in water electrolysis processes in an alkaline solution (30%wt KOH) under different current densities, using vertical stainless steel 304 electrodes (20 mm X 60 mm) with a separation of 20 mm between them in an electrolyzer made of glass (80 mm X 80 mm X 80 mm). An optical flow method is implemented to study the velocity field of hydrogen bubbles based on image sequences captured by a CCD camera with a 67.2 µm/(pixel length). In this case, the influence of current density varying between 190 and 650 A/m*^{2} *was investigated. The experimental results show that the velocity distribution in most regions of the electrolyzer is dominated by two asymmetry bubble buoyancy-induced flow patterns caused by hydrogen and oxygen plumes. The increasing velocity and vorticity fields are observed in low depth regions, generating an increase in turbulence in the electrolyte. Nevertheless, the average velocity decreases for higher current densities due to increased turbulence zones. Complex structures generated by turbulence considerably affect bubble dynamics. Such results facilitate the understanding and the dynamics of the transport phenomena of hydrogen bubbles in the electrolyzer.*

Keywords: *hydrogen generation, renewable energy, electrolysis, velocity field*

1. INTRODUCTION

Several issues involving the generation and transformation of energy have been the focus of much concern in recent years, especially with the environmental consequences. Thus, the need to generate greener forms of energy has drawn attention. A viable alternative is the generation of hydrogen through water electrolysis processes using solar panels to supply electrodes (Dincer, 2012). In fact, during the process of electrolysis of water, electrons flow through the anode to the cathode where they are incorporated by hydrogen ions to form hydrogen gas. In this way, the dissolved gas accumulates until it reaches a critical condition of supersaturated concentration at the electrode surface, initiating bubble nucleation

(Jones *et al.* (1999) and Van Damme *et al.* (2010)). Several experimental and theoretical investigations have been reported in the literature studying various aspects related to water electrolysis, including the main fluid dynamical characteristics of bubbles. Abdelouahed *et al.* (2014) studied the hydrodynamics of gas bubbles during water electrolysis using NaOH as electrolyte. The authors investigated the distributions of bubble velocities and void fractions in the anode-to-anode space. The effects of the anode gap, current density and cell inclination on the hydrodynamics of the gas phase were followed. Mohammed-Ibrahim and Moussab (2020) resumed the discussion on the use of seawater for hydrogen generation pointing out important aspects including competition of chlorine evolution reaction (ClER) with oxygen evolution reaction (OER) on the anode, salinity and temperature of the electrolyte. More recently, Lohmann-Richters *et al.* (2021) investigated the influence of temperature on increasing current density in alkaline electrolysis considering different materials for anodes and cathodes. According to the results, the increased temperature leads to significantly reduced cell voltages, which leads to increased current density and efficiency. Many researchers have also focused studies on the modeling hydrogen generation based on both theory and experimental observation (Ehrl *et al.* (2013), El-Askary *et al.* (2015), Schillings *et al.* (2015), Hreiz *et al.* (2015)), including the effect of pressure (Vogt, 2017), temperature (Olivier *et al.*, 2017), volume of hydrogen generated (Haug *et al.*, 2017). On the other hand, studies have been developed to investigate the fluid dynamic behavior of bubbles using image capture methods. Chandran *et al.* (2015) analyzed bubble size distribution of hydrogen in electrolysis using sodium chloride with horizontal electrodes. And, based on image processing, the authors obtained the relation between number of the bubbles and their diameters. An experimental investigation on bubble shape observation was performed by Jianu *et al.* (2015) during electrolysis using laser-based shadow imaging system and an on-line vapor monitoring system. The authors modeled bubble dynamics and vapor transfer kinetics considering parameters such as bubble diameter, velocity and trajectories under different operation conditions. Zhu *et al.* (2018) investigated the hydrodynamics behavior and mass transfer performance in water electrolysis processes with two configurations of containers and electrodes under different current densities. The authors used PIV method to obtain the velocity field and, according to their results, the mean vertical velocity increases with increasing current density and the natural convection is enhanced with Joule heat generation for higher current densities. Despite the several efforts reported in the literature focused on the generation and transport of hydrogen during electrolysis, understanding the bubble dynamics during this process still represents a challenge. Among the greatest difficulties is the dynamics of the two-phase flow within the electrolyte caused by the convection and vorticity zones generated by the turbulent nature of the phenomenon.

The present study has focused on the behavior of bubbles during water electrolysis thought image sequences, analyzing the velocity field and profiles as well the influence of current densities on bubble generation and transport.

2. EXPERIMENTAL FACILITY AND METHODOLOGY

Figure 1 presents the schematic of the experimental setup used to investigate the bubble dynamics. Such a setup consists of a test section which includes a cubic container with 80 mm edge, a DC power supply model Minipa MPL-3305. The working electrodes are made of stainless steel 304 (with 19% chrome and 9% nickel). The choice of this material is due to its stability in alkaline medium. Both electrodes have 30 mm wide and 70 mm long, arranged vertically with a 20 mm gap. The experiment was performed at room temperature, i.e. around 20 ^{o}C. The with a 30 %wt KOH aqueous solution in deionized water. Experimental parameters are presented in Tab. 1. All images were captured using a CCD camera model DSRL EOS with 2048 x 2048 pixel and a 50 mm lens. Based on the image resolution, the smallest length scale was 67.2 μm/pixel with a capture rate of 60 frame/s.

2.1 Chemistry of water electrolysis

The electrolyte is a dilute solution of potassium hydroxide (KOH), which disassociates into K^+ and OH^-. Thus, the oxygen gas evolves at the anode, while hydrogen gas is generated at the cathode according to the following electrochemical reaction at the anode:

$$4OH^- \rightarrow O_2(gas) + 4\bar{e} + 2H_2O \qquad (1)$$

and at the cathode:

$$4H_2O + 4\bar{e} \rightarrow 2H_2(gas) + 4OH^- \qquad (2)$$

Table 1. Experimental conditions during tests.

Properties and Parameters	Value/Range
Molar mass [mol/l]	5.34
Density of electrolyte [kg/m^3]	1237
Viscosity of electrolyte [kg/(m·s)]	0.001731
Current density [A/m^2]	190-650

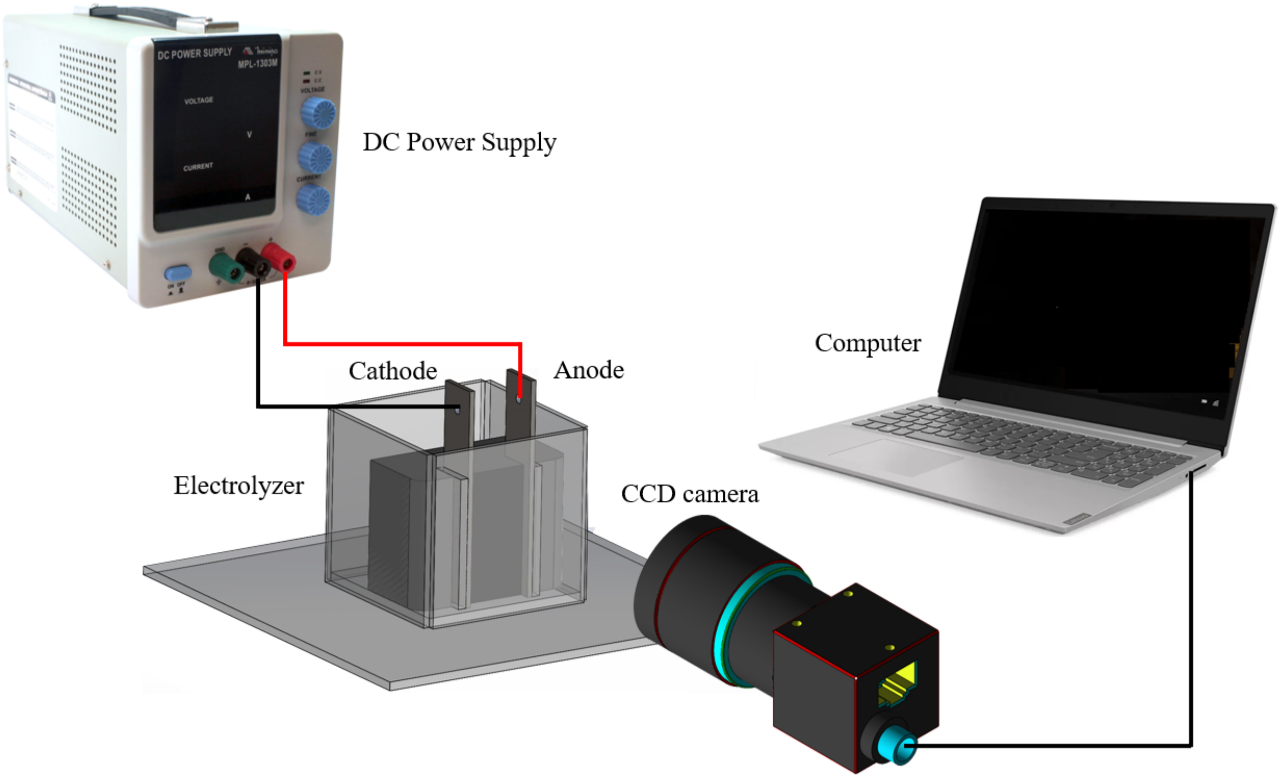

Figure 1. Experimental test rig.

2.2 Optical flow method

The optical flow is based on the method developed by Liu and Shen (2008) considering the optical flow equation for different flow visualizations, which is given in terms of image coordinates:

$$\frac{\partial g}{\partial t} + \nabla \cdot (g\mathbf{u}) = f(x, y, g) \tag{3}$$

where g represents the normalized image intensity that is proportional to the radiance received by the camera, $u = (u_x, u_y)$ is the velocity in the image plane referred to as the optical flow and $f(x, y, g)$ corresponds to a boundary and diffusion term. The optical flow u is proportional to the light-path-averaged velocity weighted with the field quantity Φ related to a visualizing medium.

A variational formulation with a smoothness constraint is used to determine the optical flow, according to a functional given by Eq. 4

$$j(\mathbf{u}) = \int_{\Omega} \left\{ \left[\frac{\partial g}{\partial t} + \nabla \cdot (g\mathbf{u}) \right]^2 + \lambda \left(|\nabla u_x|^2 + |\nabla u_y|^2 \right) \right\} dxdy \tag{4}$$

where λ corresponds to the Lagrange multiplier and Ω is an image domain. By minimizing the Eq. 4, Euler-Lagrange equation is obtained:

$$g\nabla \left[\frac{\partial g}{\partial t} + \nabla \cdot (g\mathbf{u}) - f \right] + \lambda \nabla^2 \mathbf{u} = 0 \tag{5}$$

The solution of Eq. 5 is found using the standard difference method with Neumann condition $\partial \mathbf{u}/\partial n = 0$ on the image domain.

3. RESULTS

3.1 Bubble Dynamics

Different distributions of bubbles caused by fluid dynamics can be observed during the electrolysis process, as shown in Fig. 2. Larger hydrogen bubble clusters are commonly observed at higher heights of the cathode (1), caused by regions containing greater vorticity near the electrolyte surface. Filaments of hydrogen bubbles can be observed at intermediate heights of the cathode (2). In this case, the bubbles are driven exclusively by buoyancy, causing a significant increase in the void fraction along the bubble coverage. For the case of oxygen generation, smaller bubbles are observed more dispersed from the anode (3). The smallest bubbles with a greater dispersion are, in general, observed in more centralized regions between the electrodes (4). In fact, such patterns show variations over time and electrolyte caused by the turbulent nature of bubble dynamics. The greatest influence on both the generation and the dynamics of the bubbles is caused by the current density variation (Vogt, 2013), exemplified by Fig. 3. In addition to the increase in bubble coverage along the electrode surface, an increase in the species fraction can be observed as a function of the electrode height. Such an increase is caused by the accumulation of dispersed bubbles guided by the buoyancy located both inside and outside the hydrodynamic boundary layer. Microbubbles plumes are also observed along the wall (Fig. 3(d)(e)), as well as bubbles with bigger diameters, generated by a longer residence time on the surface.

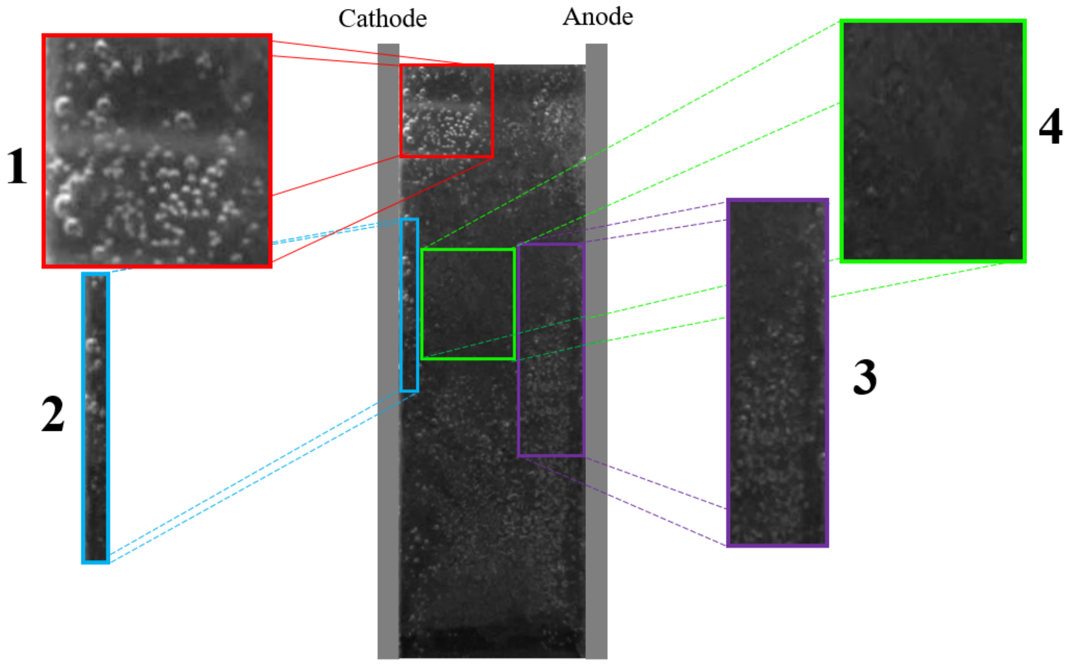

Figure 2. Characteristic bubble distribution for J = 260 A/m^2.

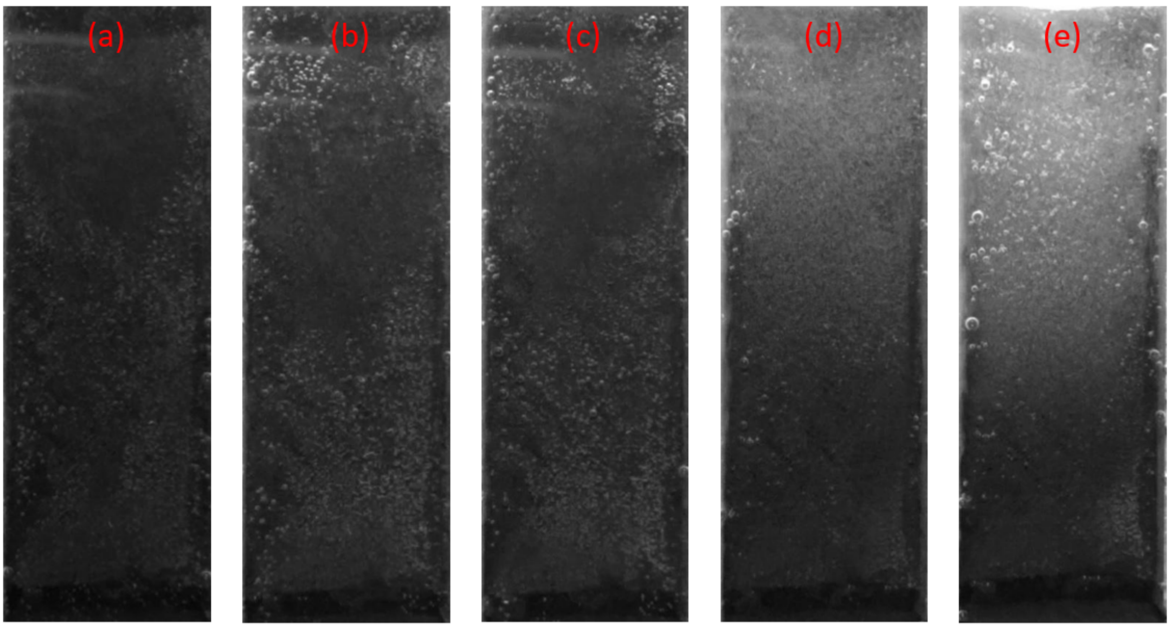

Figure 3. Images captured of bubbles for current density J of: (a) 190; (b) 260; (c) 350; (d) 530 and (e) 650 A/m^2.

3.2 Velocity Fields

Figure 4 presents an example of velocity field generated from a sequence of two imagens for J = 190 A/m^2. As it can be seen, greater intensities of velocity are observed in some regions near the cathode caused by instabilities of bubble clusters in hydrodynamic boundary layer and in regions of greater height. The greater production of bubbles is indicated by the greater intensities of velocities, causing Kelvin-Helmholtz instabilities related to variations in velocity gradients. This characteristic, in turn, generates regions of vorticity that make it difficult for the bubbles to flow and make the system more disordered and less efficient.

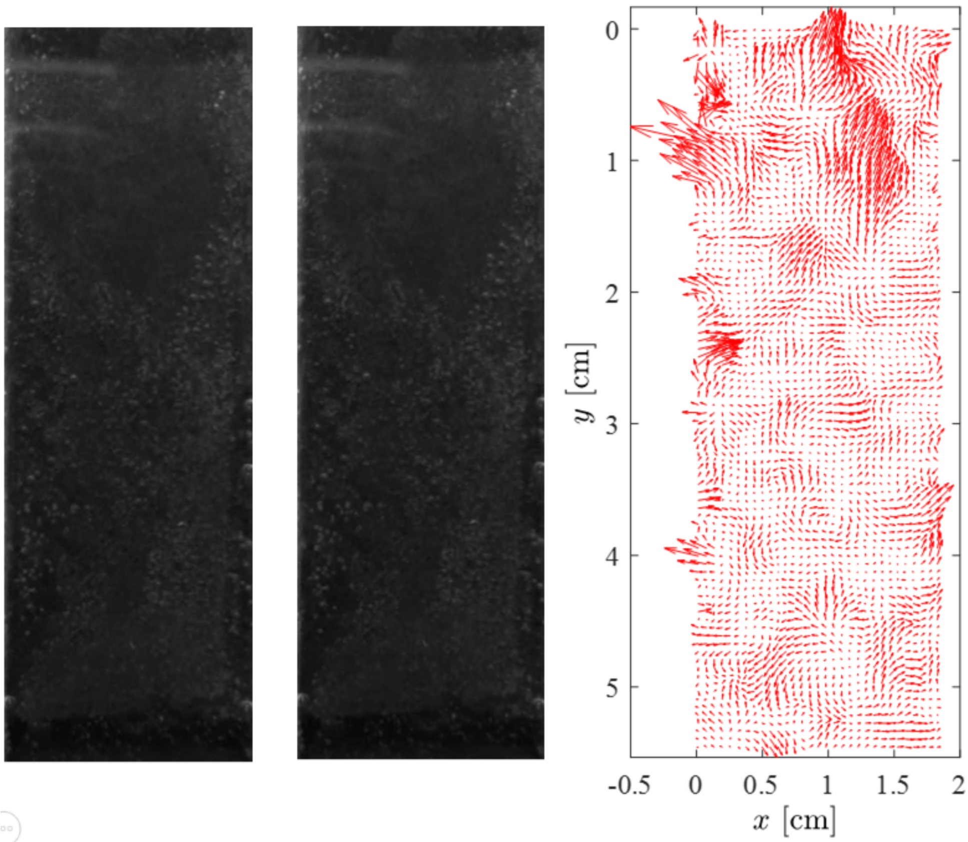

Figure 4. Velocity field generated from the sequence of images for J = 190 A/m^2.

Figure 5 shows the velocity filed from J = 190 to 530 A/m^2. It is observed that in the range from 190 A/m^2 to 530 A/m^2, there is a large increase in the velocity field, mainly in the four upper ranges of the system between 37.82 and 60 mm, where effectively the H_2 bubbles are released from the electrode and rise in surface direction with a tendency to re-unite with the O_2 bubbles generated from the anode, due to van der Waals forces. The vertical velocity profile as a function of the horizontal component x for different electrode heights is shown in Fig. 6. In all cases, the velocity profile shows fluctuations with different amplitudes caused by the flux and reflux zones of bubbles. As observed, the vertical velocity increases with increasing the current density, with $|u_y|$ varying between 1 mm/s (Fig. 6(a)) and 2.8 mm/s (Fig. 6(d)). In fact, both generation rate and consequently bubble velocity present considerable dependence on current density. Figure 7 shows the influence of current density on the absolute value of maximum velocity of bubbles. As it can be seen, such a dependence is almost linear up to 500 J/m^2, but for higher current density, the increase rate of the maximum velocity has slowed down gradually, and the increase is not linear.

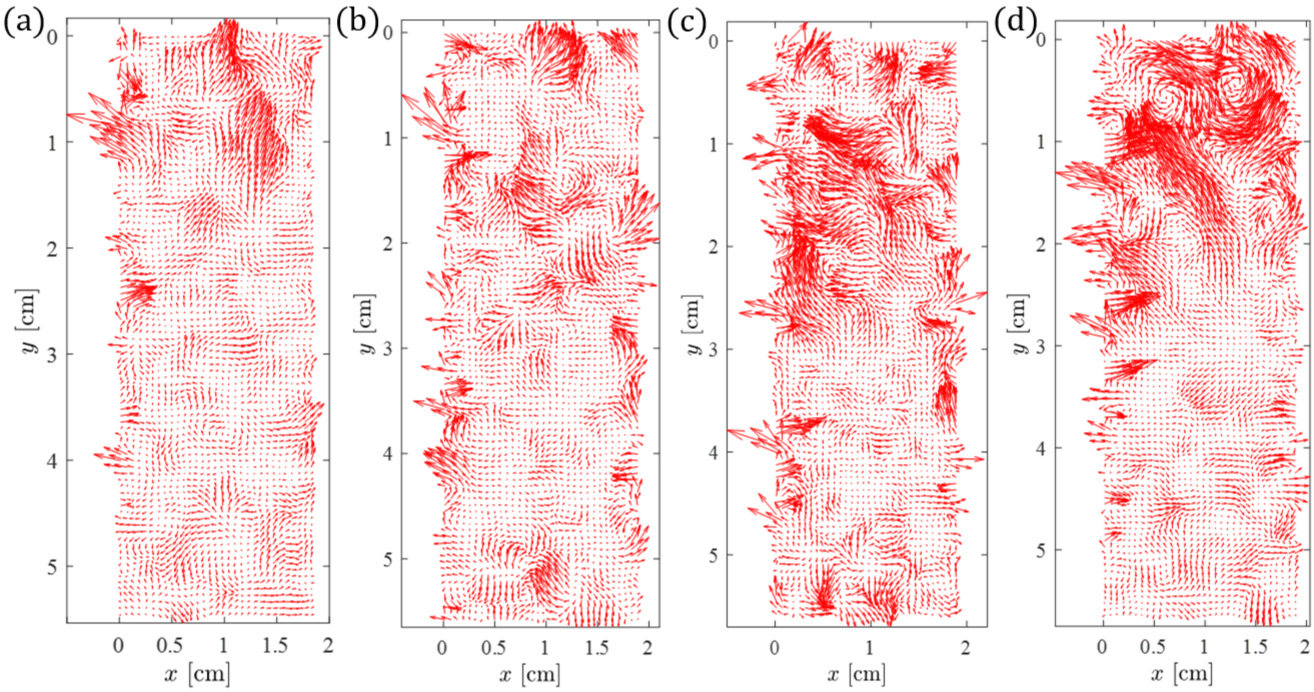

Figure 5. Velocity fields for J: (a) 190, (b) 260, (c) 350 and (d) 530 A/m^2.

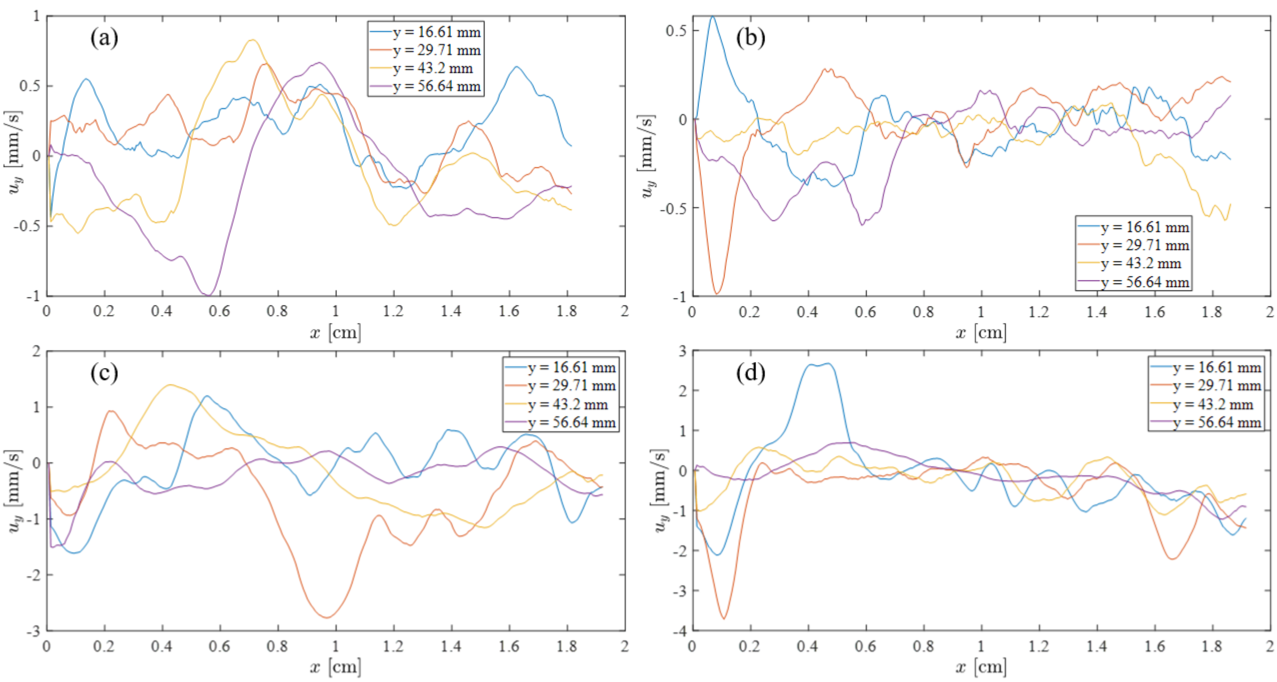

Figure 6. Vetical velocity component along the gap between electrodes for J of (a) 66 A/m^2; (b) 210 A/m^2; (c) 440 A/m^2 and (d) 650 A/m^2.

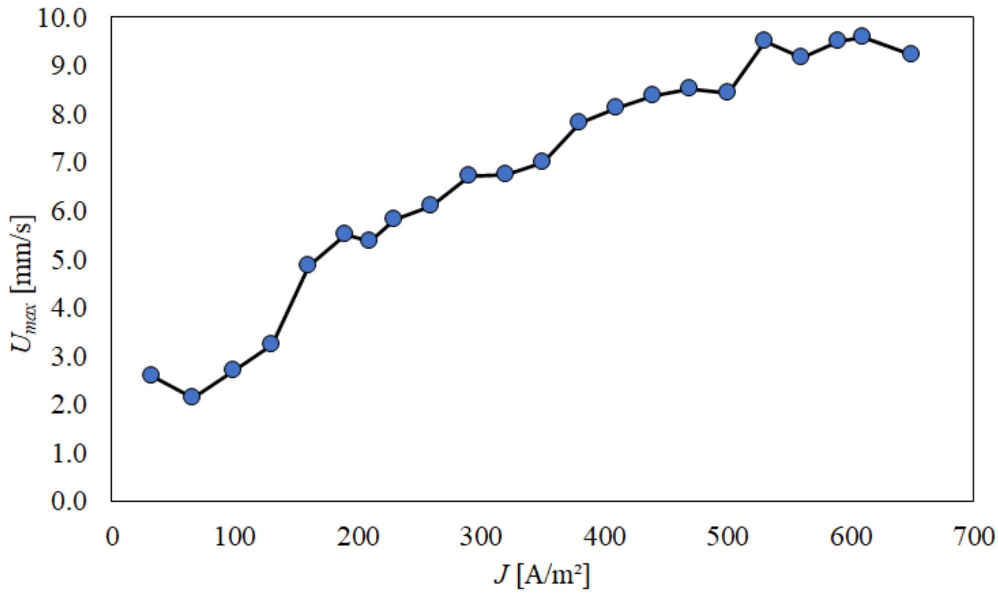

Figure 7. The maximum velocity as function of current density.

4. CONCLUSION

In this study, an experimental investigation was performed to analyse velocity fields generated by hydrogen bubbles during water electrolysis. The results show characteristics such as fluctuations of velocity fields causing vorticity between the electrodes. Such gradients are responsible for the variation in the efficiency of the electrolysis process along the electrode-electrolyte interface. It can also be observed that the greatest turbulent intensity occurs close to the electrolyte surface, causing greater difficulty in releasing hydrogen at the interface.

5. REFERENCES

Abdelouahed, L., Hreiz, R., Poncin, S., Valentin, G. and Lapicque, F., 2014. "Hydrodynamics of gas bubbles in the gap of lantern blade electrodes without forced flow of electrolyte: Experiments and cfd modelling". *Chemical Engineering Science*, Vol. 111, p. 255–265.

Chandran, P., Bakshi, S. and Chatterjee, D., 2015. "Study on the characteristics of hydrogen bubble formation and its transport during electrolysis of water". *Chemical Engineering Science journal*, Vol. 138, pp. 99–109.

Dincer, I., 2012. "Green methods for hydrogen production". *International Journal of Hydrogen Energy*, Vol. 37, p. 1954–1971.

Ehrl, A., Bauer, G., Gravemeier, V. and Wall, W.A., 2013. "A computational approach for the simulation of natural convection in electrochemical cells". *Journal of Computational Physics journal*, Vol. 235, pp. 764–785.

Eigeldinger, J. and Vogt, H., 2000. "The bubble coverage of gas–evolving electrodes in a flowing electrolyte". *Electrochimica Acta*, Vol. 45, pp. 4449–4456.

El-Askary, W.A., Sakr, I.M., Ibrahim, K.A. and Balabel, A., 2015. "Hydrodynamics characteristics of hydrogen evolution process through electrolysis: Numerical and experimental studies". *Energy*, Vol. 90, pp. 722–737.

Haug, P., Kreitz, B., Koj, M. and Turek, T., 2017. "Process modelling of an alkaline water electrolyzer". *International Journal of Hydrogen Energy*, Vol. 42, pp. 15689–15707.

Hreiz, R., Abdelouahed, L., Fünfschilling, D. and Lapicque, F., 2015. "Electrogenerated bubbles induced convection in narrow vertical cells: Piv measurements and euler–lagrange cfd simulation". *Chemical Engineering Science*, Vol. 134, pp. 138–152.

Jianu, O.A., Rosen, M.A., Naterer, G.F. and Wang, Z., 2015. "Two-phase bubble flow and convective mass transfer in water splitting processes". *International Journal of Hydrogen Energy*, Vol. 40, pp. 4047–4055.

Jones, S., Evans, G. and Galvin, K., 1999. "Bubble nucleation from gas cavities – a review". *Advances in Colloid and Interface Science*, Vol. 80, pp. 27–50.

Liu, T. and Shen, L., 2008. "Fluid flow and optical flow". *Journal of Fluid Mechanics*, Vol. 614, pp. 253–291.

Lohmann-Richters, F.P., Renz, S., Lehnert, W., Müller, M. and Carmo, M., 2021. "Review—challenges and opportunities for increased current density in alkaline electrolysis by increasing the operating temperature". *Journal of The Electrochemical Society*, Vol. 168, p. 114501.

Mohammed-Ibrahim, J. and Moussab, H., 2020. "Recent advances on hydrogen production through seawater electrolysis". *Materials Science for Energy Technologies*, Vol. 3, p. 780–807.

Olivier, P., Bourasseau, C. and Bouamama, P.B., 2017. "Low-temperature electrolysis system modelling: A review". *Renewable and Sustainable Energy Reviews*, Vol. 78, pp. 280–300.

Schillings, J., Doche, O. and Deseure, J., 2015. "Modeling of electrochemically generated bubbly flow under buoyancy-driven and forced convection". *International Journal of Heat and Mass Transfer*, Vol. 85, pp. 292–299.

Van Damme, S., Maciel, P., Parys, H.V., Deconinck, J., Hubin, A. and Deconinck, H., 2010. "Bubble nucleation algorithm for the simulation of gas evolving electrodes". *Electrochemistry Communications*, Vol. 12, p. 664–667.

Vogt, H., 2013. "Heat transfer in boiling and mass transfer in gas evolution at electrodes – the analogy and its limits". *International Journal of Heat and Mass Transfer*, Vol. 59, pp. 191–197.

Vogt, H., 2017. "The quantities affecting the bubble coverage of gas-evolving electrodes". *Electrochimica Acta*, Vol. 235, pp. 495–499.

Zhu, J., Zhang, X., Lv, P., Wang, Y. and Wang, J., 2018. "An experimental investigation of convective mass transfer characterization in two configurations of electrolysers". *International Journal of Hydrogen Energy*, Vol. 43, pp. 1–12.

6. RESPONSIBILITY NOTICE

The authors are solely responsible for the printed material included in this paper.